

Superluminous supernovae at high redshift

Tim Abbott¹, Jeff Cooke^{2,3}, Chris Curtin^{2,3}, Shahab Joudaki^{2,3}, Antonios Katsianis⁴, Anton Koekemoer⁵, Jeremy Mould^{2,3}, Edoardo Tescari^{3,6}, Syed Uddin^{2,7}, Lifan Wang⁸

¹Cerro Tololo Interamerican Observatory

²Centre for Astrophysics & Supercomputing, Swinburne University

³ARC Centre of Excellence for All-sky Astrophysics (CAASTRO)

⁴Dept of Astronomy, Universidad de Chile, Camino El Observatorio 1515, Las Condes, Santiago, Chile

⁵Space Telescope Science Institute

⁶School of Physics, University of Melbourne

⁷Purple Mountain Observatory, Chinese Academy of Sciences, Nanjing, China

⁸Texas A&M University

Abstract

Superluminous supernovae are beginning to be discovered at redshifts as early as the epoch of reionization. A number of candidate mechanisms is reviewed, together with the discovery programs.

Keywords: initial mass function – dark ages, reionization, first stars – supernovae: general – galaxies: high redshift

1 Introduction

An unavoidable problem in probing the high redshift Universe is the rapid rise of luminosity distance with redshift. In luminosity distance, the epoch of reionization (EoR) from $t = 100$ Myrs extends 80 Hubble radii. More powerful telescopes and instruments are needed for the EoR, such as: (i) JWST: [powerful, but small field, with spectroscopy paramount] (ii) DECam: [$1\mu\text{m}$ and shorter, wide field (Flaugher et al. 2012)] (iii) KDUST: [$1\mu\text{m} < \lambda < 3\mu\text{m}$, wide field (Yuan et al. 2012)] (iv) Subaru: [Hyper Suprime Cam (HSC – Miyazaki 2015)]. In this paper, we review survey successes and expectations for superluminous supernovae (SLSNe).

2 Massive and supermassive stars

We observe very massive stars ($>100 M_{\odot}$) in the present universe and, as a result, we do know that they can form. But how do they actually end their lives? Will they die as core-collapse supernovae (SNe) energized by the spin down of magnetars, pair instability supernovae (PISNe) with explosion energies up to 100 times that of regular supernovae, pulsational pair instability supernovae that can produce very bright events due to colliding shells, or via another mechanism? Asymmetry may play a critical role in evolution. Extreme events that trigger relativistic jets may become luminous enough such that their discovery can be made by relatively

small telescopes. These extreme cases may output high energy radiation as in gamma-ray bursts (GRB).

Woosley & Heger (2015) reviewed the theory of the evolution and death of stars heavier than $10 M_{\odot}$ on the main sequence. The more massive of these, absent serious mass loss, either make black holes when they die, or, for helium cores exceeding $\sim 35 M_{\odot}$, encounter the pair instability. Outcomes, including the appearance of GRBs (Levan et al 2016), depend on the initial composition of the star, its rotation rate, and detailed physics. These stars can produce some of the brightest SNe, but also some of the faintest.

Yoshida et al (2014) investigated very massive stars with main sequence mass larger than $100 M_{\odot}$ and metallicity $0.001 < Z < 0.004$ which might explode as Type Ic SLSNe. Progenitors of 43 and $61 M_{\odot}$ WO stars with $Z = 0.004$ were evolved from initial 110 and $250 M_{\odot}$ stars. These stars were expected to explode as Type Ie SNe. Other progenitor spectral types were studied by Groh et al (2013). Dessart et al (2012) point out that mixing challenges the ability to infer progenitor and explosion properties.

From the collapse of supermassive stars, supermassive black holes observed at high redshift in QSOs could grow from direct collapse black holes with mass $\sim 10^5 M_{\odot}$. Ultra-luminous supernovae (Matsumoto et al. 2016) of $\sim 10^{45-46} \text{ erg s}^{-1}$ would be detectable by future telescopes in the near infrared, such as, Euclid,

WFIRST, KDUST and JWST for ~ 5000 days to $z \lesssim 20$ and ~ 100 events per year.

The unknowns in binary massive star evolution have recently received widespread attention with the detection of a massive binary inspiral (Abbott et al. 2016a). Understanding such events in the low-redshift Universe will enable us to better interpret high redshift observations.

3 High z SNe

Does the collapse of pristine gas in the early Universe lead to the formation of very massive stars? Larson (1998), Heger & Woosley (2002), O’Shea & Norman (2007, 2008) have considered the possibility and the notion of a different initial mass function (IMF) from today’s. Wide-area, deep surveys are seeing a rare class of SLSNe, 10 – 100 times more luminous than typical SNe (Quimby et al. 2011; Gal-Yam 2012). However, only $\gtrsim 50$ SLSNe have been detected at low z (Nicholl et al 2015, Smith et al. 2007; GYL 2009; Pastorello et al. 2010; Gezari et al. 2009). One of these events with slow fade was thought to be powered by the radiative decay of ^{56}Ni (Gal-Yam et al 2009). A single event has been identified as the first detection of a third type of SN with a pair-instability supernova (PISN). As discussed above, SLSNe might to occur with higher rate at earlier times, due to the presence of pristine gas and a top-heavy IMF, which favours the creation of massive stars. Overall, according to Tescari et al (2014) and Katsianis et al (2015) an efficient feedback mechanism is needed to obtain the observed star formation rate functions and stellar mass functions at high redshifts and SLSN maybe could play a major role.

Physical models of SLSNe include pair instability supernovae (PISNe), magnetars, quark novae, radiatively shocked circumstellar matter, and jet-cocoon structures. The energy output may be as high as 10^{55-56} ergs, exceeding the main sequence radiated energy of $100 M_{\odot}$ stars at 10^{54} ergs. Models involving more than one of the concepts outlined below have been considered by Tolstov et al (2016), Gal-Yam (2016) and Gilmer et al (2016).

3.1 The PISN concept

PISNe have been theorized since the 1960s (Rakavy & Shaviv 1967; Barkat et al 1967) as the result of the deaths of stars with progenitor masses of $140-260 M_{\odot}$ (Heger & Woosley 2002; Kasen et al 2011). Stars this massive generate conditions in their cores that enable efficient conversion of γ -ray photons into electron-positron pairs, followed by rapid conversion of pressure-supporting radiation into rest mass, violent contraction

and run-away thermonuclear explosion, obliterating the star (Kozyreva et al 2017; Chatzopoulos et al 2015).

A number of events are candidates for PISN including SN2007bi (Gal-Yam et al 2009). For example, Lunnan et al (2016) discuss a number of 07bi-like PISN candidates, and they have rise photometry, one of the key discriminants. The two high redshift SLSNe of Cooke et al (2012) are perhaps the most robust PISN candidates known, in particular, the redshift 2 event.

3.2 Magnetars, quark novae

Energy injection by a magnetar with a rapid rotation rate and magnetic field of $0.1-1 \times 10^{14}$ G may supply excess luminosity. Chatzopoulos et al (2016) argue that this requires fine-tuning and extreme parameters for the magnetar, as well as the assumption of efficient conversion of magnetar energy into radiation.

Ouyed et al (2016) show that a Quark-Nova (the explosive transition of a neutron star to a quark star) occurring a few days following the SN explosion of an oxygen Wolf-Rayet star can account for SLSNe, including extreme energetics and a double-peaked light-curve. The expanding remnant is used to harness the kinetic energy ($>10^{52}$ ergs) of the ejecta.

3.3 Radiatively shocked circumstellar matter and jet-cocoon structures

Blinnikov (2016) reviews calculations, not only of the magnetar model and PISNe, but also models explaining SLSN events with the minimum energy budget, involving multiple ejections of mass in presupernova stars. The radiative shocks produced in collisions of those shells may provide the required power. This class of the models he refers to as “interacting” supernovae.

Matsumoto et al (2016) consider supermassive black holes at high redshift growing from direct collapse black holes (DCBHs) with masses $\sim 10^5 M_{\odot}$, resulting from the collapse of supermassive stars (SMSs). If a relativistic jet is launched from a DCBH, then it can break out of the collapsing SMS and produce a GRB. Although most GRB jets may miss our line of sight, they show that the energy injected from the jet into a cocoon is huge $\sim 10^{55-56}$ erg, so that the cocoon fireball is observed as an ultra-luminous supernova of $\sim 10^{45-46}$ erg/s.

4 Observing High redshift SLSNe

Two SLSNe at $z \sim 2$ have been observed: a slow evolving PISN event (Cooke et al. 2012) and another SLSN-I type event. Other surveys for high z SLSNe include the “All-Sky Automated Survey for Supernovae” (ASAS-SN; Brown & Warren-Son Holoiien 2016), the Palomar Transient Factory (Perley et al 2016), Subaru HSC surveys (Tanaka et al 2016) and GAIA (Staley & Fender

2016). The SUPERluminous Supernova Host galaxies (SUSHIES) survey (Schulze et al 2016) aims to provide constraints on the progenitors of SLSNe by understanding the relationship to their host galaxies. Appendix A reports on the DECAM Deep Fields program. Mould et al (2017) report the discovery of a $z \approx 6$ SLSN in the NSF field.

4.1 SLSN rates

The rate of core collapse SNe is proportional to the star formation rate and affected by the IMF. Many studies have been made at $z < 0.3$ (e.g., Bazin et al. 2009); few at higher z . Most core collapse SNe are too faint, although luminous type II_n and SLSNe are an exception. SLSNe are extremely luminous in the UV (Brown 2016, Yan et al 2016), whereas type Ia are not. Therefore, objects are expected to be detectable at high z . Cooke et al (2012) suggest that, at $z \sim 2-4$, the SLSN rate is $\sim 4 \times 10^{-7}$ /Mpc³/yr. This is $\lesssim 0.1\%$ of the total core collapse SN rate at $0.9 < z < 1.3$ found by Dahlen et al (2012). The z dependence of the SLSN rate has been predicted by Tanaka et al. (2012). At this rate, the surface density of SLSNe is given in column (2) of Table 1. For DECAM these objects are quite faint by redshift 4 (see column 3), but not beyond reach.

Table 1: Expected number of SLSNe/sq deg

Redshift interval	#	m-M-20
z	(deg ⁻²)	-2.5log(1+z) (mag)
(1)	(2)	(3)
(1.0, 1.5)	2	23.8
(1.5, 2.0)	2.5	24.5
(2.0, 2.5)	2.5	25.0
(2.5, 3.0)	2.5	25.4
(3.0, 3.5)	2.5	25.7
(3.5, 4.0)	2.5	25.9
(4.0, 4.5)	2.5	26.1

5 Other DECAM results

5.1 GW150914

We observed the Prime Field (Table 2) 107 days after LIGO’s first detection of a binary black hole inspiral (Abbott et al. 2016a). The error box for GW150914 includes the Prime Field. The brightest objects present after the event and not present in 2012, 2013 with colours that exclude flare stars have $z \approx 17.5$ *i.e.* $M_z \approx -20.5$ at the distance of the event. However, the binary black hole merger model predicts no electromagnetic counterpart for the event (Abbott et al 2016b). A brightening

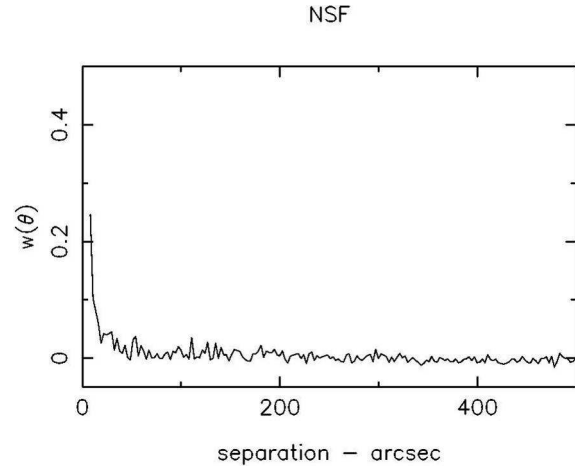


Figure 1. Angular correlation function for the NSF field. The scale at redshift 6 is 5.8 kpc/arcsec.

of at least 7.5 mag was generally seen for these objects, which were most likely SNe.

5.2 Large Scale Structure

Our first two nights of the DECAMERON project yielded data on the Prime field. Candidate i band dropouts have $z \gtrsim 6$ and their structure across the 3 square degree field is far from uniform (Figure 1). Details are given by Mould (2013). The colour-magnitude diagram was shown by Mould (2015). Figure 1 is similar to that of Barone-Nugent et al. (2014). Reionization lights up the gas on comoving scales of a few Mpc and more (Geil et al 2016). This is accessible to the DECAM Deep Field project.

5.3 Detection of SLSNe

Two of us (CC & JC) are working with SUDSS (Scovaccicchi et al. 2016), using Lyman Break Galaxy (LBG) colour cuts for $z = 3$. For present purposes, we modified these for higher redshift. The NSF field (Table 2) was drawn from SUDSS to increase the cadence. For $z = 3.5-4.8$, these cuts are $g-r > r-i + 0.8$; $g-i > 0.3$; $-0.7 < r-i < 1.2$; $-0.4 < i-z < 0.2$. These need further refinement. Figures A1-3 (Appendix A) show our $z = 4$ candidates. Mould et al (2017) report the discovery of a $z \approx 6$ SLSN in the NSF field based upon bandpass redshifts in the table below.

Table 3: Dropout bandpass vs redshift

$\lambda_{eff}/(1+z)$	
100/(1+0)	100 nm
360/(1+2.6)	<i>u</i>
480/(1+3.8)	<i>g</i>
670/(1+5.7)	<i>r</i>
820/(1+7.2)	<i>i</i>

6 Higher z (towards the Dark Ages)

There is absolutely no observational data on the stellar Universe at $z \sim 20$. Events at $z > 20$ need near infrared K-band observations. For this purpose, we can call on the low background and remarkable isoplanatism in Antarctica (Aristidi et al. 2013) to conduct wide field K-band time domain surveys. Spectroscopically, by the end of the decade we shall have JWST to detect some of these SLSNe at redshifts all the way to $z \sim 20$. While the explosion of first generation stars is of fundamental importance, the rate of SLSNe at $z \sim 20$ is highly uncertain and a low rate may limit the discovery space of JWST. The deep NIR survey to $K = 29$ th mag proposed by Wang¹ (2009) would be an excellent target feeder for JWST.

7 Conclusions

What we have seen in this brief review is a recent proliferation of SLSNe and a number of mechanisms that could be at work making them. The first four years of the DECameron project suggest that DECcam, like HSC, can penetrate the EoR. Large scale structure data are consistent with that of other programs. There is every expectation that LBG and dropout selection criteria will allow EoR SLSNe to be found. Time dilation of high z light curves allows economical observing. We plan to press on to investigate the fascinating scientific questions posed by the evolutionary end points of massive stars in the EoR. Among these are the possibility of using SLSNe for cosmology (Scovaccicchi et al 2016). The best route at higher z may be to search for ‘orphan’ SLSNe that have the correct colours and then use very deep (JWST) spectroscopy to confirm the redshift.

8 ACKNOWLEDGEMENTS

We are grateful to the DES team for building DECcam and the NVO at NOAO for flattening and stacking our data. Parts of this research were conducted by the Australian Research Council Centre of Excellence for All-sky Astrophysics (CAASTRO), through project number CE110001020. In addition to DAOPHOT, we used IRAF, a product of NOAO,

which is operated by AURA and supported by NSF. Thanks also to our colleagues Stuart Wyithe, Chris Lidman, Michele Trenti, Robert Barone Nugent and Andrea Kunder.

The DECameron project used data obtained with the Dark Energy Camera, which was constructed by the Dark Energy Survey (DES) collaboration. Funding for the DES Projects has been provided by the DOE and NSF (USA), MISE (Spain), STFC (UK), HEFCE (UK), NCSA (UIUC), KICP (U. Chicago), CCAPP (Ohio State), MIFPA (Texas A&M), CNPQ, FAPERJ, FINEP (Brazil), MINECO (Spain), DFG (Germany) and the collaborating institutions in the Dark Energy Survey, which are Argonne Lab, UC Santa Cruz, University of Cambridge, CIEMAT-Madrid, University of Chicago, University College London, DES-Brazil Consortium, University of Edinburgh, ETH Zurich, Fermilab, University of Illinois, ICE (IEEC-CSIC), IFAE Barcelona, Lawrence Berkeley Lab, LMU Munchen and the associated Excellence Cluster Universe, University of Michigan, NOAO, University of Nottingham, Ohio State University, University of Pennsylvania, University of Portsmouth, SLAC National Lab, Stanford University, University of Sussex, and Texas A&M University.

References

- Abbott, B. et al. 2016a, Phys Rev Lett, 116, 1102
 Abbott, B. et al. 2016b, ApJ, 826, L13
 Aristidi, E. et al. 2013, IAU Symposium 288, 300
 Barone-Nugent, R. et al. 2014, ApJ, 793, 17
 Barkat, Z., Rakavy, G. & Sack, N 1967, PRL, 18, 379
 Bazin, G. et al. 2009, A&A, 499, 653
 Blinnikov, S. 2016, arxiv, 1611.00513
 Brown, J. & Warren-Son Holoien, T. 2016, AAS, 227, 34913
 Brown, P. 2016, AAS, 227, 23707
 Chatzopoulos, E. et al 2015, ApJ, 799, 18
 Chatzopoulos, E. et al 2016, ApJ, 828, 94
 Cooke, J., et al. 2012, Nature, 491, 228
 Dahlen, T. et al 2012, ApJ, 757, 70
 Dessart, L. et al. 2012, MNRAS, 424, 2139
 Flaughner, B. 2012, SPIE, 8446, 11
 Gal-Yam, A. 2012, Science, 337, 927
 Gal-Yam, A. & Leonard, D. 2009, Nature, 458, 865
 Gal-Yam, A. et al. 2009, Nature, 462, 624
 Gal-Yam, A. 2016, arxiv 1611.09353
 Geil, P. et al. 2016, MNRAS, 462, 804
 Gezari, S., et al. 2009, ApJ, 690, 1313
 Gilmer, M. et al 2016, arxiv 1610.00016
 Groh, J. et al. 2013, A&A, 558, 131
 Heger, A. & Woosley, S. E. 2002, ApJ, 567, 532
 Kasen, D., Woosley, S., & Heger, A., 2011, ApJ, 734, 102
 Katsianis, A. et al. 2015, MNRAS, 448, 3001
 Kozyreva, A. et al. 2017, MNRAS, 464, 2854
 Larson, R. B., 1998, MNRAS, 301, 569
 Levan, A. et al. 2016, SSRv, 202, 33
 Lunnan, R. et al. 2016, ApJ, 831, 144
 Matsumoto, T. et al 2016, ApJ, 823, 83
 Miyazaki, S. 2015, IAUGA, 225, 5916
 Moriya, T., et al. 2016, ApJ, 833, 64
 Mould, J. 2015, ASP Conf. Ser, 491, 215
 Mould, J. et al 2017, submitted to Chinese Science Bulletin

¹ z Equals Twenty from Antarctica (zETA) program.

Mould, J. 2013, <http://www.caastro.org/reionization-in-the-red-field-presentations>. Stacking of data is carried out by the DECam community pipeline (Valdes et al. 2014). Here we report candidates for SNe at $z = 4$ in the Prime field. The light curves shown on the right are z band. Pipeline stacks are archived in 9 tiles of approximately $50'$ on a side. These tiles form a 3×3 matrix on the sky with tiles 1,5,9 as the main diagonal.

The postage stamps are Y band images. Images of the same epoch are aligned in columns. In Figures A1–3 we see supernovae that are bright in the first epoch, leaving only the host galaxy in the most recent epoch.

Nicholl, M. et al 2015, MNRAS, 452, 3869
 O’Shea, B. & Norman, M., 2007, ApJ, 654, 66
 O’Shea, B. & Norman, M., 2008, ApJ, 648, 31
 Ouyed, R. et al 2016, ApJ, in press, arxiv 1611.03657
 Pastorello, A., et al. 2010, ApJ, 724, 16
 Perley, D. et al 2016, ApJ, 830, 13
 Quimby, R. et al. 2011, Nature, 474, 487
 Rakavy, G. & Shaviv, G., 1967, ApJ, 148, 803
 Scovaccicchi, D. et al 2016, MNRAS, 456, 1700
 Smith, N., et al. 2007, ApJ, 666, 1116
 Staley, T. & Fender, R. 2016, arXiv 1606.03735
 Tanaka, M. et al. 2012, MNRAS, 422, 2675
 Tanaka, M. et al. 2016, ApJ, 819, 5
 Tescari, E. et al. 2014, MNRAS, 438, 3490
 Tolstov, A. et al. 2016, arxiv 1612.01634
 Trenti, M et al. 2010, ApJ, 714, 202
 Valdes, F. et al. 2014, ASP Conference Series 485, 379
 Wang, Lifan 2009, AAS, 213, 22604
 Woosley, S. & Heger, A. 2015, ASSL, 420, 199
 Yan, Lin et al. 2016, arXiv, 1611.02782
 Yoshida, T. et al. 2014, AIPC, 1594, 284
 Yuan, Xiangyan et al. 2013, IAUS, 288, 271

Table 2: DECamERON program

			Exp	time	kilo	secs	
Field	α, δ J2000		2012 Dec 11	2013 Jan 12	2014 May 18	2015 Jul* 23	2016 Jan ^o 1
New South -ern Field (NSF)	22:32:56 -60:33	g r i z Y			5.28 4.29 14.85	3.0 5.41 13.2 26.4	
Prime Field	5:55:07 -61:21	g r i z Y	7.2 8.4	7.8 7.8			2.0 2.025 1.65 4.95 11.55
Polar Field	16:00:00 -75:00	r i z Y			2.5 9.9 18.48 9.24	7.5 4.2	
*also 28/12	^o also 8/8						

Appendix A

Dark Energy Camera on the Blanco 4 meter telescope not only has the focal plane size the 1970s 4 meter telescopes were built for, but also has good near infrared response. The goal of the DECamERON project² is a deep wide field high redshift photometric survey to study large scale structure and rare events. It reaches M^* galaxies at redshift 6 at a wavelength of one micron, studying large scale structure and finding rare events. The aim is *not* to compete with deeper narrow surveys like BORG (Trenti et al. 2010). To maximize time allocation flexibility, all 3 of these DECam deep

²<http://astronomy.swin.edu.au/~jmould/decameron.htm>

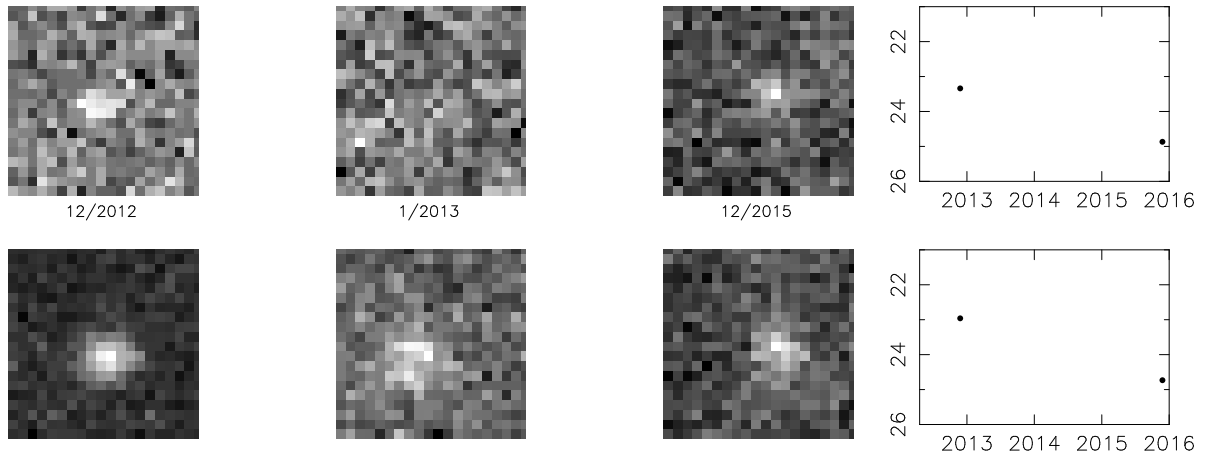


Figure A1. Tile 2 $z=4$ candidates.

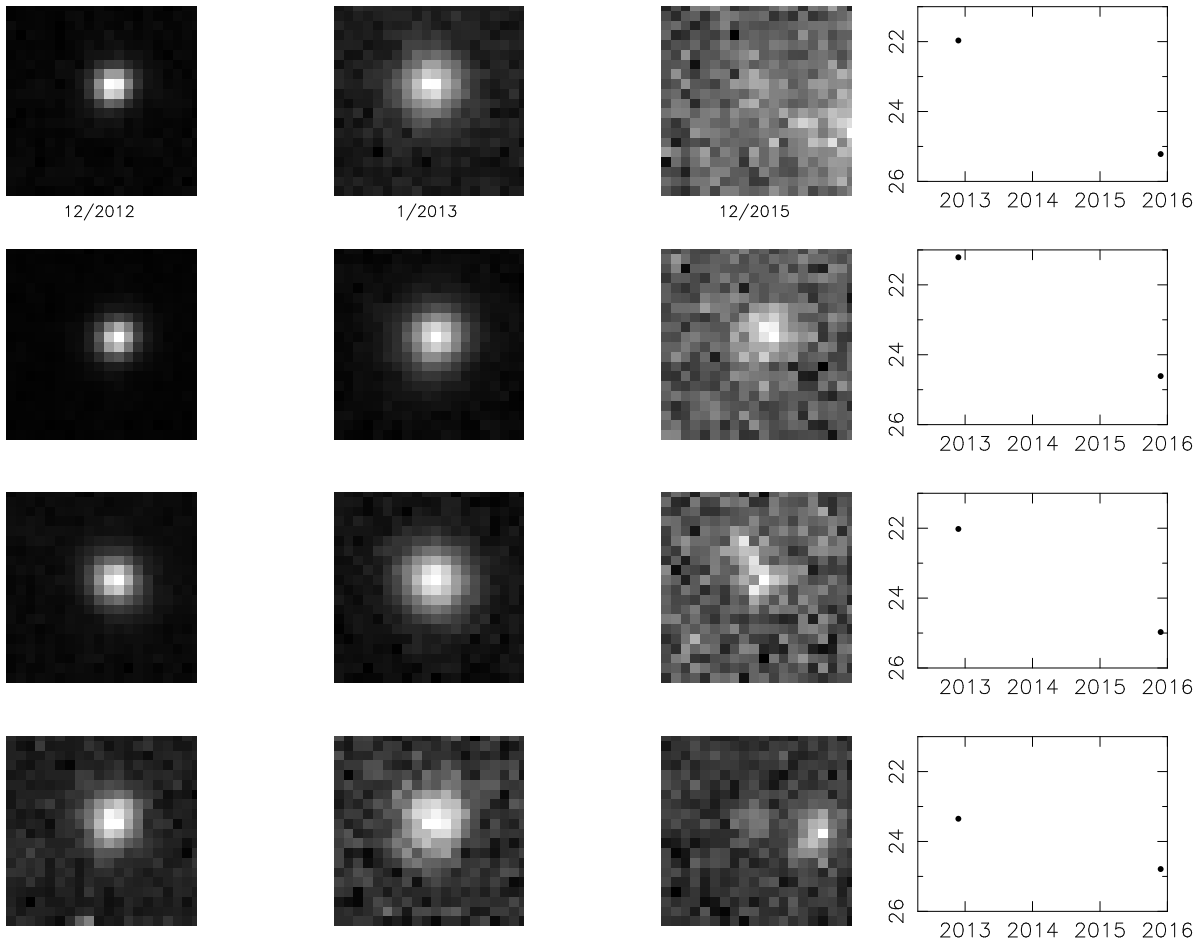


Figure A2. Tile 5 $z=4$ candidates

